RESEARCH ARTICLE

Notch receptor expression in *Trypanosoma cruzi*-infected human umbilical vein endothelial cells treated with benznidazole or simvastatin revealed by microarray analysis

Carolina Campos-Estrada[1], Fabiola González-Herrera[2], Gonzalo Greif[4], Ileana Carillo[2], Daniela Guzmán-Rivera[2], Ana Liempi[3], Carlos Robello [ID][4], Ulrike Kemmerling[3], Christian Castillo[3]* and Juan Diego Maya [ID][2]*

1 Facultad de Farmacia, Universidad de Valparaíso, Av. Gran Bretaña 1093, Playa Ancha, Valparaíso, Región de Valparaíso, 2360102, Chile
2 Programa de Farmacología Molecular y Clínica, Instituto de Ciencias Biomédicas, Facultad de Medicina, Universidad de Chile, Independencia 1027, Santiago, Región Metropolitana, 8380453, Chile
3 Programa de Biología Integrativa, Instituto de Ciencias Biomédicas, Facultad de Medicina, Universidad de Chile, Independencia 1027, Santiago, Región Metropolitana, 8380453, Chile
4 Molecular Biology Unit, Pasteur Institute and Departamento de Bioquímica, Facultad de Medicina, Universidad de la República, Avenida General Flores 2125, Montevideo, 11800, Uruguay

Abstract

Chagas disease is a vector-borne disease caused by the protozoan parasite *Trypanosoma cruzi*. Current therapy involves benznidazole. Benznidazole and other drugs can modify gene expression patterns, improving the response to the inflammatory influx induced by *T. cruzi* and decreasing the endothelial activation or immune cell recruitment, among other effects. Here, we performed a microarray analysis of human umbilical vein endothelial cells (HUVECs) treated with benznidazole and the anti-inflammatory drugs acetylsalicylic acid or simvastatin and infected with *T. cruzi*. Parasitic infection produces differential expression of a set of genes in HUVECs treated with benznidazole alone or a combination with simvastatin or acetylsalicylic acid. The differentially expressed genes were involved in inflammation, adhesion, cardiac function, and remodeling. Notch1 and high mobility group B1 were genes of interest in this analysis due to their importance in placental development, cardiac development, and inflammation. Quantitative polymerase chain reaction confirmation of these two genes indicated that both are upregulated in the presence of benznidazole.

Keywords: benznidazole; endothelial cells; Notch1; simvastatin; *Trypanosoma cruzi*

Introduction

Chagas disease affects the heart and gastrointestinal tract and is responsible for a high disease burden and mortality in Latin America. Although pharmacological strategies against the vector-borne hemoflagellate protozoan *Trypanosoma cruzi* have been intensively studied (Perez-Molina and Molina, 2018), there have been no advances in the clinical introduction of new agents that are more effective than the current conventional therapy. The nitroheterocyclic derivatives benznidazole (Bz) and nifurtimox are useful in the management of the acute phase of the disease, primarily when used in the pediatric population. In adults and chronic cases, the efficacy is low, and adherence to treatment decreases due to appearance of severe adverse reactions (Bern, 2015).

Chronic Chagas heart disease (CCHD) is the leading cause of death in 30% of patients with untreated Chagas disease (Bonney et al., 2019). Although elimination of the parasite is key to halting the progression of this disease, different clinical studies have not provided sufficient evidence to demonstrate a positive impact on CCHD progression (Morillo et al., 2015).

Thus, it is essential to determine the pathophysiology of this disease to identify therapeutic strategies that modify the host's physiopathological factors to improve conventional trypanocidal therapy with Bz (Bonney et al., 2019). The persistence of the parasite in cardiac tissue is the primary factor leading a pathophysiological process that ends in heart failure, arrhythmias, and apical aneurysm,

causing death in these patients. These manifestations are due to a chronic inflammatory process (Rassi et al., 2017). As part of these inflammatory processes, endothelial activation is observed, along with high expression of endothelial adhesion molecules that facilitate the recruitment of leukocytes that infiltrate the cardiac muscle (Campos-Estrada et al., 2015). In addition, there is an increase in the production of thromboxane and platelet aggregation and the generation of local microthrombi and focal areas of ischemia, which may contribute to the appearance of fibrous tissue by myofibroblasts. All of these alterations contribute, at least in part, to the structural changes in chronic Chagas cardiomyopathy (CCC), such as thinning of the ventricular wall and conduction disorders (Echeverria and Morillo, 2019).

Previously, our group reported that acetylsalicylic acid (ASA) and simvastatin (Simv) modulate the expression of adhesion molecules in endothelial cells infected with *T. cruzi* (Molina-Berrios et al., 2013a, b; Campos-Estrada et al., 2015). Through this effect, the recruitment of inflammatory cells in infected tissues can be reduced. Such an effect was observed in a murine model of chronic chagasic heart disease. In that model, inflammatory cell infiltration decreased when the mice were treated with these two drugs. However, it is not clear whether ASA or Simv, alone or in combination with Bz, affects the expression of endothelial adhesion molecules by modulating gene expression or by post-transcriptional effects (Campos-Estrada et al., 2015). Moreover, treating human umbilical vein endothelial cells (HUVECs) with anti-inflammatory or trypanocidal drugs before the *T. cruzi* challenge allows us to determine, to some extent, the conditions during parasite dissemination throughout treatment; such conditions might occur after a late diagnosis of the disease (Campos-Estrada et al., 2015). Throughout the infective process, during the acute and chronic phases, the cells are infected in a nonuniform manner; however, there is an inconstant but permanent spread of the parasite, from infected to uninfected cells, which may be near or far. Therefore, in this context, a trypanocidal drug might change the genetic programming, anticipating what will ensue when the parasite contacts the host cell.

Thus, a transcriptomic study was carried out on HUVECs treated with these drugs and infected with *T. cruzi* to determine the effect on the messenger RNA (mRNA) expression of adhesion molecules in this particular setting.

In addition to the results obtained for the genes related to the adhesion molecules, a striking effect was also found in the expression of the Notch receptor. Although some previous data have linked the expression of the Notch receptor to inflammatory processes that are also typical in *T. cruzi* infection (Nagajyothi et al., 2009), we report here the expression of Notch in the context of the use of agents with anti-inflammatory properties. Therefore, the Notch pathway may be modulated pharmacologically to favorably alter host responses to *T. cruzi* infection.

Methods

Cell culture

HUVECs were maintained in cell culture media 200 supplemented with low serum growth supplement and fetal bovine serum (2% v/v) (Thermo Fisher Scientific, USA). HUVECs (1.5×10^6 cells) were seeded in 75 cm^2 multiwell plates for 24 h. After incubation with 20 μM Bz, 5 μM Simv, 125 μM ASA, or 10 μM Bz/1 μM Simv or 10 μM Bz/40 μM ASA combinations for another 24 h, the cells were washed with sterile phosphate-buffered saline to remove dead cell debris and were infected with *T. cruzi* trypomastigotes (DM28c strain) at a cell:parasite ratio of 1:10 for 16 h. Finally, the HUVECs were harvested by trypsinization and stored in RNALater (Sigma-Aldrich, USA) until RNA isolation. Cells without parasites or pharmacological treatment were used as uninfected controls.

RNA isolation

Total RNA was isolated with a Total RNA Isolation Mini-Kit (Agilent Technologies, USA) according to the manufacturer's instructions. The RNA concentration and purity were quantified by spectrophotometry (NanoDrop 2000/2000c spectrophotometer; Thermo Fisher Scientific), and A260/A280 values between 1.9 and 2.0 were obtained. To assess the RNA integrity, we performed microchip capillary electrophoresis (Bioanalyzer 2100; Agilent Technologies, USA) to obtain the RNA integrity number (RIN), where a RIN of 1 indicates degraded RNA and a RIN of 10 indicates perfectly conserved RNA. The RIN values for all samples were above 9.

Microarray procedure

Complementary DNA (cDNA) was generated from 200 ng of total RNA by reverse-transcription and transcribed back to complementary RNA (cRNA) to generate Cy3-labeled RNA according to the Low Input Quick Amp-One Color Labeling Kit (Agilent Technologies). The total yield of Cy3-labeled cRNA was purified with an Illustra RNAspin Mini Isolation kit (GE Healthcare, USA), and the Qubit RNA HS kit (Thermo Fisher Scientific) was used for quantification. Hybridization with SurePrint G3 Human GE 8×60K chips (Agilent Technologies) was performed for 17 h at 60°C in an Agilent hybridization oven at 10 rpm.

Table 1 Quantitative reverse-transcription polymerase chain reaction (RT-qPCR) primer sequences.

Genes	Forward (5′–3′)	Reverse (5′–3′)
Notch-1	ACCCTTTTCTGGGGAAAGACACTG	GGCTCTGGCAAGTCTCCTACAAAA
Notch-2	CTGTTTCACTCACTCACCCAGCAT	CCCTTGGGCTAAGGAAAGTTCAGT
Notch-3	ATTCGGCCAAGCTGGATTCTGT	CATGTCCCATCTGGAATGCAGTGA
Notch-4	GCTACGATGGACAGAACTGCTCAA	GTTTGGGAGTACAGGTTCCATGGT
Hey-1	TTGTGACAGCCCTGATTCAGAT	TCAAAGTAACCTTGGTCTCCCG
PSEN1	CGGGGAAGCGTATACCTAATCT	ACGGTGCAGGTAACTCTGTC
JAG1	CTGCCTTTCAGTTTCGCCTG	ACTGTCAGGTTGAACGGTGTC
HES1	GCACAGAAAGTCATCAAAGCCT	GAGTGCGCACCTCGGTATTA
GAPDH	AAAGCCTGCCGGTGACTAAC	CCCAATACGACCAAATCAGAGAATA

The instructions of Agilent's Low Input Quick Amp Labeling Kit were followed for washing, stabilization, and drying of microarray chips.

Chips were scanned in a G256BA Agilent microarray scanner, and the data were collected with Agilent Feature Extraction (version 9.5.1), which was also used for quality control, data filtering, and normalization. Data generated from the microarray experiments were analyzed with GeneSpring GX 13 software. Fold changes ≥2 and $P \leq 0.05$ indicated differential expression. Analysis of variance (ANOVA) followed by the Benjamini–Hochberg false discovery rate correction for multiple testing was used for statistical analysis.

Real-time quantitative reverse-transcription polymerase chain reaction (RT-qPCR) validation

cDNA was obtained from 400 ng of total RNA using an M-MLV Reverse Transcriptase Kit and Oligo(dT) primers (Sigma-Aldrich). Sensifast qPCR Master Mix (Bioline, UK) was used for the RT-qPCR reactions. For each reaction, 100 mM of forward and reverse primers was mixed with 1 μL of cDNA and analyzed in an ABI7300 Real-Time thermocycler (Applied Biosystems) with cycles of 95°C for 10 s, 60°C and 15 s of annealing, and a final extension step of 72°C for 10 s. The hGAPDH gene was used as housekeeping gene, and the values were determined by the $\Delta\Delta C_t$ method (Pfaffl, 2001). The sequences for all primers are detailed in Table 1. The results were compared to those of the uninfected control and are expressed as the mean ± standard deviation. ANOVA and Dunnett's post-test statistics were used to test significance.

Results

T. cruzi infection and pharmacological pretreatment result in a differential expression profile in HUVECs

Hybridization with the SurePrint G3 Human GE 8 × 60K chip allows the analysis of at least 26K genes. In the current setup, only those genes that displayed at least a twofold change with a 95% chance to be differentially expressed were selected ($P \leq 0.05$) (Dembele and Kastner, 2014). As depicted in Figure 1, *T. cruzi* infection of HUVECs upregulated 159 genes and downregulated 242 genes. However, the assessed treatments resulted in few upregulated genes, while the Sim/Bz combination induced more upregulated genes than infection alone or both drugs separately. However, the downregulated genes induced by all the treatments outnumbered those decreased by the effect of the infection, except for the drug combination.

A selection of the most upregulated and downregulated genes (fold change range between 2.03 to 72.70 and −22.37 to −44.28, respectively) during *T. cruzi* infection is shown in Table 2. From the differentially expressed genes, relevant genes related to the immune response (CSF2, CCL2, CXCL11, CXCL2, CCL19, NLRC5, NLRC3, and HMGB1), adhesion/cell interaction processes (ICAM1, VCAM, LGALS9C, PANX3, and SELE), cardiac function (FOXH1), and remodeling (ELN, TIMP3, and KRTAP6-3) were selected.
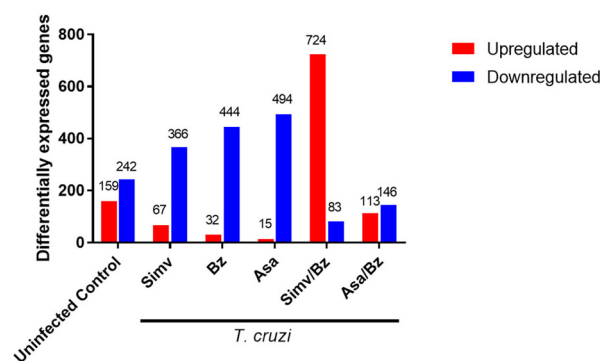

Figure 1 Differential gene expression in *Trypanosoma cruzi*-infected human umbilical vein endothelial cells (HUVECs) 16 h postinfection. HUVECs were pretreated with simvastatin (Simv), benznidazole (Bz), aspirin (ASA), Simv/Bz, or ASA/Bz and infected with *T. cruzi* trypomastigotes for 16 h. Genes with fold changes ≥2 and $P \leq 0.05$ were considered differentially expressed. Red bars indicate upregulated genes and blue bars indicate downregulated genes.

Table 2 Gene expression changes in human umbilical vein endothelial cells (HUVEC) cells infected with *Trypanosoma cruzi*.

Immune response

Gene symbol	Description	Fold change
CSF2	*Homo sapiens* colony-stimulating factor 2 (granulocyte-macrophage) (CSF2), mRNA [NM_000758]	72.70
IFITM1	*H. sapiens* interferon-induced transmembrane protein 1 (IFITM1), mRNA [NM_003641]	60.94
CCL2	*H. sapiens* chemokine (C-C motif) ligand 2 (CCL2), mRNA [NM_002982]	58.51
IFIT5	*H. sapiens* interferon-induced protein with tetratricopeptide repeats 5 (IFIT5), mRNA [NM_012420]	41.27
CXCL11	*H. sapiens* chemokine (C-X-C motif) ligand 11 (CXCL11), mRNA [NM_005409]	35.95
NID2	*H. sapiens* nidogen 2 (osteonidogen) (NID2), mRNA [NM_007361]	34.80
IL4I1	*H. sapiens* interleukin 4-induced 1 (IL4I1), transcript variant 1, mRNA [NM_152899]	31.51
IRF9	*H. sapiens* interferon regulatory factor 9 (IRF9), mRNA [NM_006084]	30.90
CXCL2	*H. sapiens* chemokine (C-X-C motif) ligand 2 (CXCL2), mRNA [NM_002089]	27.83
STAT1	*H. sapiens* signal transducer and activator of transcription 1, 91 kDa (STAT1), transcript variant β, mRNA [NM_139266]	27.59
SAMD9L	*H. sapiens* sterile α motif domain-containing 9-like (SAMD9L), mRNA [NM_152703]	27.27
DDX58	*H. sapiens* DEAD (Asp-Glu-Ala-Asp) box polypeptide 58 (DDX58), mRNA [NM_014314]	26.99
EIF2AK2	*H. sapiens* eukaryotic translation initiation factor 2-alpha kinase 2 (EIF2AK2), transcript variant 3, mRNA [NM_001135652]	26.83
GAL	*H. sapiens* galanin/GMAP prepropeptide (GAL), mRNA [NM_015973]	25.16
HMHA1	*H. sapiens* histocompatibility (minor) HA-1 (HMHA1), transcript variant 1, mRNA [NM_012292]	24.57
F2RL3	*H. sapiens* coagulation factor II (thrombin) receptor-like 3 (F2RL3), mRNA [NM_003950]	24.25
SPSB2	*H. sapiens* splA/ryanodine receptor domain and SOCS box containing 2 (SPSB2), transcript variant 1, mRNA [NM_032641]	22.72
CNTF	*H. sapiens* ciliary neurotrophic factor (CNTF), mRNA [NM_000614]	22.69
IFI6	*H. sapiens* interferon, α-inducible protein 6 (IFI6), transcript variant 3, mRNA [NM_022873]	8.13
CCL19	*H. sapiens* chemokine (C-C motif) ligand 19 (CCL19), mRNA [NM_006274]	5.86
TRAF1	*H. sapiens* TNF receptor-associated factor 1 (TRAF1), transcript variant 1, mRNA [NM_005658]	7.61
IFI44	*H. sapiens* interferon-induced protein 44 (IFI44), mRNA [NM_006417]	4.66
IFI27	*H. sapiens* interferon, α-inducible protein 27 (IFI27), transcript variant 2, mRNA [NM_005532]	4.45
ZC3HAV1	*H. sapiens* zinc finger CCCH-type, antiviral 1 (ZC3HAV1), transcript variant 2, mRNA [NM_024625]	2.40
NLRC5	*H. sapiens* NLR family, CARD domain containing 5 (NLRC5), mRNA [NM_032206]	4.13
ISG20	*H. sapiens* interferon stimulated exonuclease gene 20 kDa (ISG20), mRNA [NM_002201]	2.15
GZMB	*H. sapiens* granzyme B (granzyme 2, cytotoxic T-lymphocyte-associated serine esterase 1) (GZMB), mRNA [NM_004131]	−22.69
HMGB1	*H. sapiens* high mobility group box 1 (HMGB1), mRNA [NM_002128]	1.77
NLRC3	NLR family, CARD domain containing 3 [Source:HGNC Symbol;Acc:29889] [ENST00000324659]	44.28
	Adhesion/interaction	
LGALS9C	*H. sapiens* lectin, galactoside-binding, soluble, 9C (LGALS9C), mRNA [NM_001040078]	36.84
GPC4	*H. sapiens* glypican 4 (GPC4), mRNA [NM_001448]	24.00
PANX3	*H. sapiens* pannexin 3 (PANX3), mRNA [NM_052959]	22.92
JAM2	*H. sapiens* junctional adhesion molecule 2 (JAM2), transcript variant 3, mRNA [NM_001270408]	22.56
LGALS9	*H. sapiens* lectin, galactoside-binding, soluble, 9 (LGALS9), transcript variant 1, mRNA [NM_009587]	19.03
ICAM1	*H. sapiens* intercellular adhesion molecule 1 (ICAM1), mRNA [NM_000201]	5.13
VCAM1	*H. sapiens* vascular cell adhesion molecule 1 (VCAM1), transcript variant 1, mRNA [NM_001078]	4.85
ISG15	*H. sapiens* ISG15 ubiquitin-like modifier (ISG15), mRNA [NM_005101]	4.63
C2CD4B	*H. sapiens* C2 calcium-dependent domain containing 4B (C2CD4B), mRNA [NM_001007595]	3.37
SELE	*H. sapiens* selectin E (SELE), mRNA [NM_000450]	2.03
	Cardiac function	
GPCPD1	*H. sapiens* glycerophosphocholine phosphodiesterase GDE1 homolog (S. cerevisiae) (GPCPD1), mRNA [NM_019593]	22.04

(Continued)

Table 2 (Continued)

Immune response

Gene symbol	Description	Fold change
NOV	*H. sapiens* nephroblastoma overexpressed (NOV), mRNA [NM_002514]	46.70
FOXH1	*H. sapiens* forkhead box H1 (FOXH1), mRNA [NM_003923]	−22.37
	Remodelation	
ELN	*H. sapiens* elastin (ELN), transcript variant 1, mRNA [NM_000501]	35.23
KRTAP19-7	*H. sapiens* keratin-associated protein 19-7 (KRTAP19-7), mRNA [NM_181614]	9.22
TIMP3	*H. sapiens* TIMP metallopeptidase inhibitor 3 (TIMP3), mRNA [NM_000362]	3.38
PARP14	*H. sapiens* poly(ADP-ribose) polymerase family, member 14 (PARP14), mRNA [NM_017554]	2.76
KRTAP6-3	*H. sapiens* keratin-associated protein 6-3 (KRTAP6-3), mRNA [NM_181605]	2.54
MRAS	*H. sapiens* muscle RAS oncogene homolog (MRAS), transcript variant 1, mRNA [NM_012219]	2.44

mRNA, messenger RNA.

Infection also determines the upregulation of several pathways involved in the biological response to infection, such as the G protein-coupled receptor signaling pathway. Interestingly, changes in pathways related to the immune response were also observed, such as the upregulation of type II interferon signaling, IFN-α/β signaling, and Toll-like receptor signaling. There were fewer downregulated pathways in response to *T. cruzi* infection, but processes related to G-protein-coupled receptors, potassium channels, ACE inhibitor pathways, RAGE signaling, and cell differentiation were identified (Table 3). However, for the gene analysis, the relative weight of individual genes on each signaling pathway was weak (Table 3).

Table 3 List of upregulated and downregulated pathways in human umbilical vein endothelial cells (HUVECs) infected with *Trypanosoma cruzi*.

	P value	Matched entities	Pathway entities of experiment type
Upregulated pathways			
Hs GPCR downstream signaling	1.64E+02	11	406
Hs GPCR ligand binding	7.45E+02	11	371
Hs interferon alpha-beta signaling	0	10	45
Hs type II interferon signaling (IFNG)	0	9	37
Hs RIG-I-MDA5 mediated induction of IFN-alpha-beta pathways	1.49E+00	7	56
Hs GPCRs, class A rhodopsin-like	0.01059428	6	262
Hs gastrin-CREB signaling pathway via PKC and MAPK	5.58E+03	6	147
Hs regulation of toll-like receptor signaling pathway	0.00334297	5	150
Hs TWEAK signaling pathway	1.33E+02	5	42
Hs neurotransmitter receptor binding and downstream transmission in the postsynaptic cell	0.01126321	4	124
Hs Toll-like receptor signaling pathway	0.00555981	4	102
Hs selenium pathway	0.00305412	4	83
Hs folate metabolism	0.00130155	4	66
Hs RANKL-RANK signaling pathway	6.94E+02	4	55
Hs vitamin B12 metabolism	4.82E+02	4	53
Hs immunoregulatory interactions between a lymphoid and a non-lymphoid cell	0.0049799	3	292
Downregulated pathways			
Hs peptide GPCRs	0.01741871	2	74
Hs potassium channels	0.03230865	2	99
Hs ACE inhibitor pathway	0.0470987	1	17
Hs advanced glycosylation end product receptor signaling	0.03347929	1	13
Hs cell differentiation-index	0.03621853	1	54

Table 4 Upregulated genes with FC > 5 in infected cells pre-treated with Bz, Simv, or Asa.

FC	Gene symbol	Description
	Bz	
15.86	SLC7A10	*Homo sapiens* solute carrier family 7 (neutral amino acid transporter light chain, asc system), member 10 (SLC7A10),
10.45	CRYBA4	*H. sapiens* crystallin, beta A4
6.18	IL1R2	*H. sapiens* interleukin 1 receptor, type II (IL1R2), transcript variant 1, mRNA [NM_004633]
5.23	NOTCH1	*H. sapiens* notch 1 (NOTCH1), mRNA [NM_017617]
	Simv	
11.45	AMTN	*H. sapiens* amelotin (AMTN), transcript variant 1, mRNA [NM_212557]
10.23	AOC1	*H. sapiens* amine oxidase, copper containing 1 (AOC1), transcript variant 2, mRNA [NM_001091]
10.09	RD3	*H. sapiens* retinal degeneration 3 (RD3), transcript variant 1, mRNA [NM_183059]
9.91	CSAG3	*H. sapiens* CSAG family, member 3 (CSAG3), transcript variant 2, mRNA [NM_001129828]
7.23	CDH6	Cadherin 6, type 2, K-cadherin (fetal kidney) [Source:HGNC Symbol;Acc:1765] [ENST00000506396]
6.58	TNNT1	*H. sapiens* troponin T type 1 (skeletal, slow) (TNNT1), transcript variant 4, mRNA [NM_001291774]
6.19	HTN3	*H. sapiens* histatin 3 (HTN3), mRNA [NM_000200]
	Asa	
19.22	AMICA1	*H. sapiens* cDNA FLJ33028 fis, clone THYMU2000140. [AK057590]
15.00	JADE2	*H. sapiens* jade family PHD finger 2 (JADE2), transcript variant 3, mRNA [NM_015288]
6.97	IL6ST	*H. sapiens* interleukin 6 signal transducer (IL6ST), transcript variant 3, mRNA [NM_001190981]
5.96	SIGLECL1	*H. sapiens* SIGLEC family like 1 (SIGLECL1), transcript variant 1, mRNA [NM_173635]

Asa, acetylsalicylic acid; Bz, benznidazole; cDNA, complementary DNA; mRNA, messenger RNA; Simv, simvastatin.

Effect of the Bz, Simv, and ASA treatments on the gene expression of *T. cruzi*-infected HUVECs

Table 4 shows genes with a FC in expression >5 when the HUVECs were treated with Bz, Simv, or ASA. Bz treatment induced upregulation of the amino acid transporter SLC7A10, the crystallin protein CRYBA4, the interleukin 1 receptor IL1R2, and the NOTCH1 signaling pathway. Simv upregulated amelotin (AMTN), the metal-binding membrane glycoprotein AOC1, the retinal degeneration protein RD3, the CSAG3 gene, the cadherin CDH6, the troponin TNNT1, and histatin 3 (HTN3). Finally, ASA upregulated the adhesion molecule AMICA1, the finger protein JADE, the IL-6 signal transducer IL6ST, and SIGLEC family like 1 (SIGLECL1).

We also analyzed commonly up- or downregulated genes following the Bz, Simv, or ASA treatments and the Bz/Simv or Bz/ASA combinations (Table 5). Although the analysis of commonly upregulated genes with the three treatments showed changes in the mRNA levels of CC2D1B, Q4S4D0, HAUS3, and CNIH2, NOTCH1 expression was the most relevant in the Bz or Simv/Bz treatment modalities.

Bz treatment increases Notch 1 expression in HUVECs in response to *T. cruzi* infection

To further validate Notch 1 upregulation, we performed RT-qPCR under the same experimental conditions, and the mRNA levels of Notch 1, 2, 3, and 4; Hey1; Hes1; PSEN1; and JAG1 were determined (Figures 2 and S2). *T. cruzi* infection increased the mRNA levels of Notch1 by 55% (which was not significant), Notch 2 (51%), and Notch 3 (314%, $P \le 0.001$),

but the Notch 4 mRNA levels decreased by 49% ($P \le 0.05$). Compared with infection/no treatment, Bz treatment increased the Notch 1 mRNA levels (241%, $P \le 0.001$) but decreased the Notch 2 and Notch 3 mRNA levels by 60% ($P \le 0.001$) and 75% ($P \le 0.01$), respectively. The Simv, ASA, Bz/Simv, and Bz/ASA treatments did not affect Notch1 expression (Figure 2B). The mRNA levels of Notch 2 were decreased by the Bz or Simv treatments ($P \le 0.001$ and $P \le 0.05$, respectively), but neither the Bz/Simv nor the Bz/ASA combinations modified its expression (Figure 2C). For Notch 3, Bz, Simv, and ASA decreased its expression by 74.8%, 57.9% and 75%, respectively ($P \le 0.001$) (Figure 2D). Notch 4 expression was not affected by the individual treatments or their combinations (Figure 2E).

The mRNA levels of the HEY1 transcription factor increased in the Bz-treated infected cells by 301% ($P \le 0.001$), Simv-treated cells by 290% ($P \le 0.001$), and ASA-treated cells by 330% ($P \le 0.001$); however, neither Bz/Simv nor Bz/ASA altered HEY1 expression (Figure 2 F). For HES1, only the ASA and Bz/ASA treatments increased its mRNA expression (128% and 110%, respectively, $P \le 0.01$ and 0.05) (Figure 2G). Neither *PSN1* nor *JAG1* showed relevant changes in the expression (Figures 2H–I).

Although microarrays for uninfected, treated HUVECs are lacking, qPCR validation was performed for the genes of the Notch pathway in these cells (Figure S2). In these settings, simvastatin alone increased Notch 1 mRNA; however, the Notch1 pathway reporters did not increase under the present experimental conditions. Strikingly, Notch 2 mRNA increased with Bz, ASA and Simv but not with the combinations. Finally, HES increased only

Table 5 Fold change in common upregulated genes after drug treatments

Gene symbol	Description	FC Bz/Inf	FC Simv/Inf	FC Comb
	BZ/Simv common upregulated genes			
CC2D1B	*Homo sapiens* coiled-coil and C2 domain containing 1B (CC2D1B), mRNA [NM_032449]	4.94	4.38	3.90
HAUS3	*H. sapiens* HAUS augmin-like complex, subunit 3 (HAUS3), mRNA [NM_024511]	2.00	2.08	2.54
NOTCH1	*H. sapiens* notch 1 (NOTCH1), mRNA [NM_017617]	5.23	1.54	2.37
	BZ/Asa common upregulated genes			
CNIH2	*H. sapiens* cornichon family AMPA receptor auxiliary protein 2 (CNIH2), transcript variant 1, mRNA [NM_182553]	2.40	2.51	3.21
CC2D1B	*H. sapiens* coiled-coil and C2 domain containing 1B (CC2D1B), mRNA [NM_032449]	4.94	2.70	2.82
	Bz, Simv, Asa common upregulated genes			
CC2D1B	*H. sapiens* coiled-coil and C2 domain containing 1B (CC2D1B), mRNA [NM_032449]	4.94	4.38	2.69
Q4S4D0	Q4S4D0_TETNG (Q4S4D0) chromosome 2 SCAF14738 (Fragment), partial (3%) [THC2574155]	3.54	4.41	5.63

Asa, acetylsalicylic acid; Bz, benznidazole; mRNA, messenger RNA; Simv, simvastatin.

with the combination of Bz and ASA; however, HEY1 mRNA was not detected in any of the conditions.

Discussion

T. cruzi persistence is the central determinant for chronicity and the adverse structural consequences in the myocardium (Viotti et al., 2014). Under these circumstances, permanent inflammation induces fibrosis and ultimately leads to tissue dysfunction causing the typical manifestations of CCC, such as heart failure and, eventually, death (Bonney et al., 2019). However, as part of chronic inflammation, several immune and repair processes occur, introducing a high level of complexity to *T. cruzi*-induced cardiac tissue damage (Echeverria and Morillo, 2019). Thus, understanding the mechanisms involved in the development of CCC is necessary
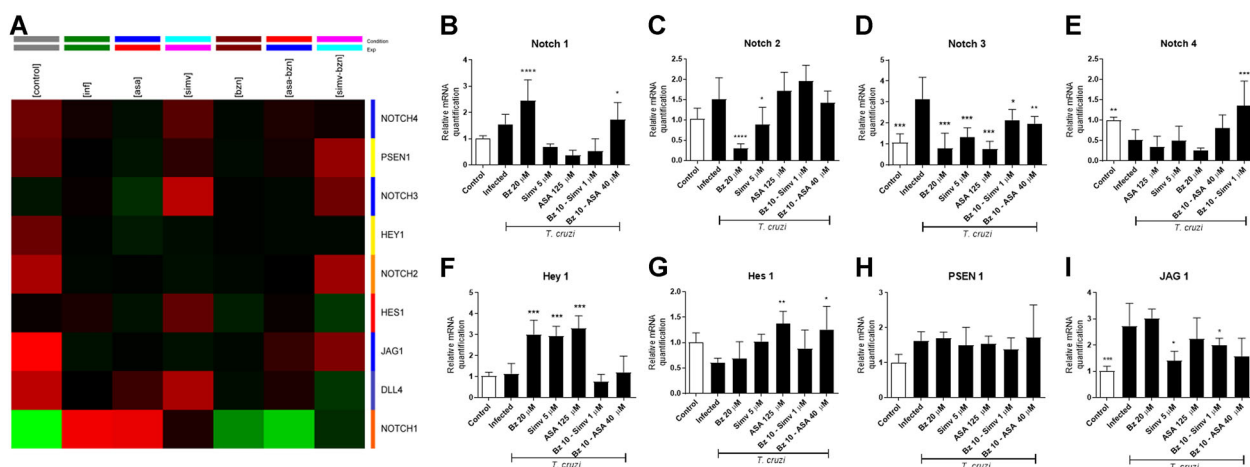

Figure 2 *Trypanosoma cruzi* infection induces Notch 1 expression in human umbilical vein endothelial cells (HUVECs). HUVECs were infected with *T. cruzi* trypomastigotes or treated with benznidazole (Bz), simvastatin (Simv), aspirin (ASA), or Bz/Simv-Bz/ASA combinations. A heatmap of the NOTCH pathway microarray is shown in (A). The expression of Notch1–4 (B–E), Hey1 (F), Hes1 (G), PSEN1 (H), and JAG1 (I) was assayed by quantitative reverse-transcription polymerase chain reaction (RT-qPCR). Values were normalized to those of hGAPDH and compared with *T. cruzi*-infected untreated controls. The statistical significance of the data was analyzed by analysis of variance followed by Dunnett's post-test. *$P < 0.05$, **$P < 0.01$, ***$P < 0.001$.

to develop new diagnostic methods as well as new therapeutic strategies. Moreover, pretreating HUVECs before challenging them with the parasite allows analysis of the conditions underlying infection spread, which might occur both during both the acute and chronic stages of the disease. Thus, gene programming may differ from that occurring after the amastigotes are established in the host cell followed by antichagasic treatment.

Undoubtedly, *T. cruzi* infection produces significant changes in cellular gene expression, as shown in several reports (Manque et al., 2011; Chiribao et al., 2014; Li et al., 2016). These findings were also observed in our model, where 159 genes were upregulated and 242 were down-regulated during the infection. Notably, the treatments used herein did not affect the parasite load, as previously reported (Campos-Estrada et al., 2015).

As expected, immune response-related genes were increased by the 16-h *T. cruzi* infection. This finding is reinforced by the upregulation of related pathways, such as type II interferon signaling, IFN-α/β signaling, and Toll-like receptors. Moreover, CCL2, CXCL11, and other related chemokines were shown to be increased during infection with *T. cruzi* in heart and immune cells, including cardiomyocytes and macrophages, respectively (Graefe et al., 2006; Horta et al., 2018). Although the role of NLRC5 in *T. cruzi* infection has not been investigated, the role of Nod-like receptors in the regulation of the inflammasome has attracted some attention due to the potential to regulate the burden of infection through innate immunity (Gurung and Kanneganti, 2016). Similarly, in the innate immune response to *T. cruzi*, only the parasite homolog for the high mobility group box 1 (TcHMGB1) has been characterized as a proinflammatory factor (Tavernelli et al., 2019); however, this is the first report of host-derived HMGB1, as depicted in Figure S1. The HMGB1 protein is a nuclear nonhistone protein that is generally involved in cellular proliferation and differentiation processes. Pathogen recognition receptor activation induces extracellular translocation of this protein, where it acts as an alarmin, participating in cell signaling and inflammation (Andersson et al., 2018).

Cell adhesion molecules (CAMs) are necessary to allow the transit of immune cells from the blood to infected tissues. Thus, activated endothelial cells are important in inflammation as they express these adhesion molecules. This is the reason why ICAM and VCAM genes are upregulated in HUVECs after *T. cruzi* infection, and this finding agreed with previous reports showing that CAMs are increased in *T. cruzi*-infected endothelial cells (Molina-Berrios et al., 2013, 2013).

Although Castillo et al. (2018) previously reported changes similar to those described in the present model, the number of downregulated genes was high compared with that observed by Chiribao et al. (2014). That study found a high number of differentially expressed genes

(1700) when the effect of infection on epithelial cells was analyzed. However, although the experimental conditions of the infection were similar to those of the present report, the cell type was different, and the infection time was longer. Therefore, the response time is fundamental when performing an analysis of these characteristics. When the infection is already established, with no intracellular duplication of the parasite, the list of genes modified as a result of reprogramming could be smaller. Indeed, as reported by Li et al. (2016), the most relevant transcriptomic changes occur in the early stages of intracellular infection, in parallel with the transformation of the parasite into an amastigote. Once amastigote maturity is reached, the transcriptomic changes stabilize. Therefore, it is possible that the initial gene response would maintain the infection on the one hand and mount an immune response to eliminate the parasite on the other. This last response would eventually be responsible for the inflammation induced by the presence of the parasite. Thus, the initial gene reprogramming would establish a balance between the permanence of the parasite and the efforts of the host to eliminate it.

Bz and Simv also modulate immune response genes and pathways. This finding is not surprising because Bz has an anti-inflammatory effect by itself (Lambertucci et al., 2017). Simv may also modify inflammation through the production of COX_2-derived 15-epi-lipoxin A_4 and modulation of the NFκB pathway (Tousoulis et al., 2014), as reported for hearts chronically infected with *T. cruzi* (Campos-Estrada et al., 2015). In the current treatment settings, the upregulation of a set of immune genes was limited, possibly because HUVECs are not specialized immune cells or because the time for drug incubation was not enough to observe a more extensive number of genes. Nevertheless, endothelial cells are capable of producing cytokines, interleukins, and adhesion molecules when a noxious stimulus is present, which is necessary for immune cell infiltration in the pathogen-exposed tissue.

One of the most interesting events observed during gene reprogramming with Bz was the increased expression of the Notch1 receptor gene.

In embryos, the Notch signaling pathways function mainly in heart morphogenesis and coronary angiogenesis (Quillard and Charreau, 2013; Luxan et al., 2016a, b). In adults, this pathway may contribute to endothelial barrier maintenance and regulate angiogenesis (Zhou et al., 2018). However, since all its components are present, it can be activated after the appearance of specific stressors, which in the heart can be ischemia (Li et al., 2010). Furthermore, in some experimental models, Notch regulates fibrotic remodeling after ischemic insult (Nistri et al., 2017). It is postulated that during cardiac ischemic processes, such as acute myocardial infarction, there is a notch-driven trend

toward increasing cardiac progenitor cell differentiation. Most likely, this process will replace lost cardiomyocytes, decrease conversion from fibroblasts to myofibroblasts, and promote collateral vessels by angiogenesis, as a part of the overall effort to further reduce the scar area (Zhou et al., 2018).

There are four Notch receptors (Notch1–4) and five ligands (Jagged 1 and 2, Delta-like 1, 3, and 4), which have a broad combinatory potential, leading to distinct responses. The Notch-ligand proteins, expressed on a neighboring cell, trigger the canonical Notch signaling pathway. Successive proteolytic cleavages, controlled by a γ-secretase, lead to a fragment (the intracellular domain) that translocates to the nucleus and interacts with a transcriptional repressor called recombination-signal-binding protein for the immunoglobulin-kJ region (RBP-J) in the CSL complex (CBF1/RBP-j/Su(H)/Lag-1) (Iso et al., 2003). Consequently, RBP-J is converted from a repressor to a transcriptional activator regulating the expression of Notch-dependent genes, such as members of the Hes and Hey gene families or members of the nuclear factor-κB (NF-κB) pathway (Luxan et al., 2016). These genes are involved in the regulation of several developmental processes, such as proliferation, cell differentiation, apoptosis, adhesion, and epithelial-to-mesenchymal transition, in a broad range of cell types, as well as homeostasis of self-renewing tissues during adult life (Cuman et al., 2014).

Notch participates in vascular inflammation, inflammatory cytokine release, atherosclerotic plaque formation, and activated macrophage infiltration (Aquila et al., 2013). However, its activity in endothelial cells is necessary for the prevention of remodeling and protection of the endothelium under conditions such as inflammation and ischemia (Ferrari and Rizzo, 2014). In the injured myocardium, Notch has a regulatory role in the functional recovery of the ischemic myocardium, reactivating developmental processes in the adult. Under these circumstances, Notch reduces myocardial ischemia-reperfusion injury by (i) limiting myocyte hypertrophy, (ii) enhancing myocyte survival, (iii) promoting precursor proliferation, (iv) controlling cardiogenic differentiation, and (v) reducing interstitial fibrosis (Nistri et al., 2017). Thus, pharmacological modulation of Notch signaling should decrease endothelial inflammation and enhance neovascularization and perfusion recovery for inflammatory and ischemic heart diseases (Rizzo et al., 2014). Under *T. cruzi* infection, the Notch1 receptor is upregulated, although marginally, after treatment with the combination of Bz/ASA. Moreover, *T. cruzi* counteracts the effects of Simv to increase Notch1 mRNA production. HEY1 upregulation was also observed with the Bz, Simv, and ASA treatments; however, it decreased in the absence of the parasite.

The combination of Bz and ASA increased the expression of HES1, but this effect was independent of the infection. Overall, Notch 3 and Notch 4 expressions were unaffected by the treatments or the presence of *T. cruzi*. Notably, the most important variable in the present analysis is the parasite and how it can modify cell programming. The intracellular host environment changes as the cell is exposed to both Bz, Simv, or ASA and the parasite together. A microarray analysis would be desirable; however, the qPCR validation of uninfected, treated controls provides a sound baseline for comparisons.

Therefore, in the context of CCC, notch pathway modulation could have beneficial effects, promoting differentiation from mesenchymal cells to cardiomyocytes, favoring angiogenesis, and consequently improving cardiac perfusion (Ferrari and Rizzo, 2014). This assertion is supported by reports indicating that Notch 1 promotes the differentiation of mesenchymal cells from the bone marrow to cardiomyocytes (Yu et al., 2016). In addition, Boopathy et al. (2015) reported that intracardiac administration of jagged 1, one of Notch's ligands, decreased ischemia-induced fibrosis in a model of acute myocardial infarction. In either case, more studies are needed, as there are reports that Notch activation can also induce reparative fibrosis (Russell et al., 2011).

Bz, and probably ASA, may allow intercellular communication preventing the transformation of fibroblasts into myofibroblasts. Thus, fibrosis decreases, and damaged cardiomyocytes are replaced with new compromised cardiac pluripotent cells. Although still controversial, Bz may play an important role in the course of CCC because of its anti-inflammatory actions. Bz itself decreased NF-kB and MAPK activation and liver inflammation in a mouse-induced sepsis model (Ronco et al., 2011), probably through the induction of nuclear factor erythroid-derived 2-like and decreased expression and therefore localization of TLR4 in the membrane (Lambertucci et al., 2017), partly explaining its anti-inflammatory action. However, it has been reported that although Bz decreases the parasitic load in animal models of CCC, it cannot reverse or improve the structural damage induced by the parasite and therefore does not prevent the development of cardiomyopathy (Santos et al., 2012, 2016). This evidence is complemented by studies in humans where Bz was unable to reverse cardiac alterations in previously treated patients (Molina et al., 2014; Morillo et al., 2015). However, a recent report by Camara et al. (2019) described the preservation of myocardial function in patients treated with Bz associated with a potentially protective increase in IL-17.

ASA and Bz may modulate Notch pathway activation to induce a reparative process decreasing the progression of the cardiac damage induced by fibrosis secondary to chronic inflammation. Thus, a synergistic effect may ensure

that Bz also has trypanocidal effects that will clear persistent parasites in the tissue. The Notch pathway is activated during inflammation, as was reported in adipose tissue infected by *T. cruzi*. However, this pathway might be modified favorably to alter the course of the disease. Further confirmation of this hypothesis is needed, but the Notch 1 pathway is an attractive candidate for drug modulation of the natural disease course.

Conclusion

T. cruzi can modulate the molecules involved in inflammatory processes. Additionally, in HUVECs previously treated with Bz, ASA, or Simv, induction of the genes involved in the Notch1 pathway could be observed, which was confirmed by PCR. Pharmacological modulation of this pathway may be beneficial for CCC therapy.

Acknowledgments and funding

Author contribution

C.C.-E.: performed the microarray experiments, gene expression database construction, and data analysis of the results. F.G., I.C.: performed the qPCR experiments and analysis of the results and discussion. G.G.: performed the microarray experiments and gene expression database construction. D.G. and A.L. performed the HUVEC cultures and incubation with parasites and drugs and discussed the results. C.R.: performed the microarray experiments and database construction and contributed to the discussion and manuscript editing. U.K.: performed the microarray experiments and database construction and contributed to the discussion and manuscript editing. C.C. and J.D.M. performed the microarray experiments, database construction, analysis and discussion of the results and manuscript redaction.

Conflict of interest

The authors declare no conflicts of interest.

Data availability

Databases generated during the current study are available at the GEO repository, accession number GSE128270: https://www.ncbi.nlm.nih.gov/geo/query/acc.cgi?acc=GSE128270.

References

Andersson U, Yang H, Harris H (2018) High-mobility group box 1 protein (HMGB1) operates as an alarmin outside as well as inside cells. Semin Immunol 38: 40–8, https://doi.org/10.1016/j.smim.2018.02.011

Aquila G, Pannella M, Morelli MB, Caliceti C, Fortini C, Rizzo P, Ferrari R (2013) The role of Notch pathway in cardiovascular diseases. Glob Cardiol Sci Pract 2013(4): 364–71, https://doi.org/10.5339/gscp.2013.44

Bern C (2015) Chagas' disease. N Engl J Med 373(5): 456–66, https://doi.org/10.1056/NEJMra1410150

Bonney KM, Luthringer DJ, Kim SA, Garg NJ, Engman DM (2019) Pathology and pathogenesis of chagas heart disease. Annu Rev Pathol 14: 421–47, https://doi.org/10.1146/annurev-pathol-020117-043711

Boopathy A, Martinez M, Smith A, Brown M, García A, Davis M (2015) Intramyocardial delivery of Notch ligand-containing hydrogels improves cardiac function and angiogenesis following infarction. Tissue Eng Part A 21(18): 2315–22, https://doi.org/10.1089/ten.TEA.2014.0622

Camara EJN, Mendonca VRR, Souza LCL, Carvalho JS, Lessa RA, Gatto R, Barreto LO, Chiacchio G, Amarante E, Cunha M, Alves-Silva LS, Guimarães BAC, Barral-Netto M (2019) Elevated IL-17 levels and echocardiographic signs of preserved myocardial function in benznidazole-treated individuals with chronic Chagas' disease. Int J Infect Dis 79: 123–30, https://doi.org/10.1016/j.ijid.2018.11.369

Campos-Estrada C, Liempi A, Gonzalez-Herrera F, Lapier M, Kemmerling U, Pesce B, Ferreira J, López-Muñoz R, Maya JD (2015) Simvastatin and benznidazole-mediated prevention of trypanosoma cruzi-induced endothelial activation: role of 15-epi-lipoxin A4 in the action of simvastatin. PLoS Negl Trop Dis 9(5): e0003770, https://doi.org/10.1371/journal.pntd.0003770

Castillo C, Carrillo I, Libisch G, Juiz N, Schijman A, Robello C, Kemmerling U (2018) Host-parasite interaction: changes in human placental gene expression induced by *Trypanosoma cruzi*. Parasit Vectors 11(1): 479, https://doi.org/10.1186/s13071-018-2988-0

Chiribao ML, Libisch G, Parodi-Talice A, Robello C (2014) Early *Trypanosoma cruzi* infection reprograms human epithelial cells. BioMed Res Int 2014: 439501–12, https://doi.org/10.1155/2014/439501

Cuman C, Menkhorst E, Winship A, Van Sinderen M, Osianlis T, Rombauts LJ, Dimitriadis E (2014) Fetal-maternal communication: the role of Notch signalling in embryo implantation. Reproduction 147(3): R75–86, https://doi.org/10.1530/REP-13-0474

Dembele D, Kastner P (2014) Fold change rank ordering statistics: a new method for detecting differentially expressed genes. BMC Bioinformatics 15: 14, https://doi.org/10.1186/1471-2105-15-14

Echeverria LE, Morillo CA (2019) American trypanosomiasis (Chagas disease). Infect Dis Clin North Am 33(1): 119–34, https://doi.org/10.1016/j.idc.2018.10.015

Ferrari R, Rizzo P (2014) The Notch pathway: a novel target for myocardial remodelling therapy? Eur Heart J 35(32): 2140–45, https://doi.org/10.1093/eurheartj/ehu244

Graefe SE, Streichert T, Budde BS, Nurnberg P, Steeg C, Muller-Myhsok B, Fleischer B (2006) Genes from Chagas susceptibility loci that are differentially expressed in *T. cruzi*-resistant mice are candidates accounting for impaired immunity. PLoS One 1: e57, https://doi.org/10.1371/journal.pone.0000057

Gurung P, Kanneganti TD (2016) Immune responses against protozoan parasites: a focus on the emerging role of Nod-like receptors. Cell Mol Life Sci 73(16): 3035–51, https://doi.org/10.1007/s00018-016-2212-3

Horta AL, Figueiredo VP, Leite ALJ, Costa GP, Menezes APJ, Ramos CO, Pedrosa TCF, Bezerra FS, Vieira PMA, Talvani A (2018) The beta-blocker carvedilol and the benznidazole modulate the cardiac immune response in the acute infection induced by Colombian strain of the *Trypanosoma cruzi*. Mem Inst Oswaldo Cruz 113(11): e180271, https://doi.org/10.1590/0074-02760180271

Iso T, Hamamori Y, Kedes L (2003) Notch signaling in vascular development. Arterioscler Thromb Vasc Biol 23(4): 543–53, https://doi.org/10.1161/01.ATV.0000060892.81529.8F

Lambertucci F, Motino O, Villar S, Rigalli JP, de Lujan Alvarez M, Catania VA, Martín-Sanz P, Carnovale CE, Quiroga AD, Francés DE, Ronco MT (2017) Benznidazole, the trypanocidal drug used for Chagas disease, induces hepatic NRF2 activation and attenuates the inflammatory response in a murine model of sepsis. Toxicol Appl Pharmacol 315: 12–22, https://doi.org/10.1016/j.taap.2016.11.015

Li Y, Hiroi Y, Liao JK (2010) Notch signaling as an important mediator of cardiac repair and regeneration after myocardial infarction. Trends Cardiovasc Med 20(7): 228–31, https://doi.org/10.1016/j.tcm.2011.11.006

Li Y, Shah-Simpson S, Okrah K, Belew AT, Choi J, Caradonna KL, Padmanabhan P, Ndegwa DM, Temanni MR, Corrada Bravo H, El-Sayed NM, Burleigh BA (2016) Transcriptome remodeling in *Trypanosoma cruzi* and human cells during intracellular infection. PLoS Pathog 12(4): e1005511, https://doi.org/10.1371/journal.ppat.1005511

Luxan G, D'Amato G, MacGrogan D, de la Pompa JL (2016a) Endocardial Notch signaling in cardiac development and disease. Circ Res 118(1): e1–e18, https://doi.org/10.1161/CIRCRESAHA.115.305350

Luxan G, D'Amato G, de la Pompa JL (2016b) Intercellular Signaling in Cardiac Development and Disease: The NOTCH pathway. In: Nakanishi T, Markwald RR, Baldwin HS, Keller BB, Srivastava D et al., eds. *Etiology and morphogenesis of congenital heart disease: from gene function and cellular interaction to morphology*. Tokyo: Springer, pp. 103–114.

Manque PA, Probst CM, Pereira MC, Rampazzo RC, Ozaki LS, Pavoni DP, Silva Neto DT, Carvalho MR, Xu P, Serrano MG, Alves JM, Meirelles Mde N, Goldenberg S, Krieger MA, Buck GA (2011) *Trypanosoma cruzi* infection induces a global host cell response in cardiomyocytes. Infect Immun 79(5): 1855–62, https://doi.org/10.1128/IAI.00643-10

Molina I, Gomez i Prat J, Salvador F, Trevino B, Sulleiro E, Serre N, Pou D, Roure S, Cabezos J, Valerio L, Blanco-Grau A, Sánchez-Montalvá A, Vidal X, Pahissa A (2014) Randomized trial of posaconazole and benznidazole for chronic Chagas' disease. N Engl J Med 370(20): 1899–908, https://doi.org/10.1056/NEJMoa1313122

Molina-Berrios A, Campos-Estrada C, Lapier M, Duaso J, Kemmerling U, Galanti N, Leiva M, Ferreira J, López-Muñoz R, Maya JD (2013a) Benznidazole prevents endothelial damage in an experimental model of Chagas disease. Acta Trop 127(1): 6–13, https://doi.org/10.1016/j.actatropica.2013.03.006

Molina-Berrios A, Campos-Estrada C, Lapier M, Duaso J, Kemmerling U, Galanti N, Ferreira J, Morello A, López-Muñoz R, Maya JD (2013b) Protection of vascular endothelium by aspirin in a murine model of chronic Chagas' disease. Parasitol Res 112(7): 2731–39, https://doi.org/10.1007/s00436-013-3444-x

Morillo CA, Marin-Neto JA, Avezum A, Sosa-Estani S, Rassi A, Jr., Rosas F, Villena E, Quiroz R, Bonilla R, Britto C, Guhl F, Velazquez E, Bonilla L, Meeks B, Rao-Melacini P, Pogue J, Mattos A, Lazdins J, Rassi A, Connolly SJ, Yusuf S, BENEFIT Investigators (2015) Randomized trial of benznidazole for chronic Chagas' cardiomyopathy. N Engl J Med 373(14): 1295–306, https://doi.org/10.1056/NEJMoa1507574

Nagajyothi F, Desruisseaux MS, Weiss LM, Chua S, Albanese C, Machado FS, Esper L, Lisanti MP, Teixeira MM, Scherer PE, Tanowitz HB (2009) Chagas disease, adipose tissue and the metabolic syndrome. Mem Inst Oswaldo Cruz 104(Suppl 1): 219–25.

Nistri S, Sassoli C, Bani D (2017) Notch signaling in ischemic damage and fibrosis: evidence and clues from the heart. Front Pharmacol 8: 187, https://doi.org/10.3389/fphar.2017.00187

Pérez-Molina JA, Molina I (2018) Chagas disease. The Lancet 391(10115): 82–94, https://doi.org/10.1016/s0140-6736(17)31612-4

Pfaffl MW (2001) A new mathematical model for relative quantification in real-time RT-PCR. Nucleic Acids Res 29(9): 45, https://doi.org/10.1093/nar/29.9.e45

Quillard T, Charreau B (2013) Impact of notch signaling on inflammatory responses in cardiovascular disorders. Int J Mol Sci 14(4): 6863–88, https://doi.org/10.3390/ijms14046863

Rassi A, Jr., Marin JAN, Rassi A (2017) Chronic Chagas cardiomyopathy: a review of the main pathogenic mechanisms and the efficacy of aetiological treatment following the benznidazole evaluation for interrupting trypanosomiasis (BENEFIT) trial. Mem Inst Oswaldo Cruz 112(3): 224–35, https://doi.org/10.1590/0074-02760160334

Rizzo P, Mele D, Caliceti C, Pannella M, Fortini C, Clementz AG, Morelli MB, Aquila G, Ameri P, Ferrari R (2014) The role of notch in the cardiovascular system: potential adverse effects of investigational notch inhibitors. Front Oncol 4: 384, https://doi.org/10.3389/fonc.2014.00384

Ronco MT, Manarin R, Frances D, Serra E, Revelli S, Carnovale C (2011) Benznidazole treatment attenuates liver NF-kappaB

activity and MAPK in a cecal ligation and puncture model of sepsis. Mol Immunol 48(6–7): 867–73, https://doi.org/10.1016/j.molimm.2010.12.021

Russell JL, Goetsch SC, Gaiano NR, Hill JA, Olson EN, Schneider JW (2011) A dynamic notch injury response activates epicardium and contributes to fibrosis repair. Circ Res 108(1): 51–9, https://doi.org/10.1161/CIRCRESAHA.110.233262

Santos FM, Lima WG, Gravel AS, Martins TA, Talvani A, Torres RM, Bahia MT (2012) Cardiomyopathy prognosis after benznidazole treatment in chronic canine Chagas' disease. J Antimicrob Chemother 67(8): 1987–95, https://doi.org/10.1093/jac/dks135

Santos FM, Mazzeti AL, Caldas S, Goncalves KR, Lima WG, Torres RM, Bahia MT (2016) Chagas cardiomyopathy: the potential effect of benznidazole treatment on diastolic dysfunction and cardiac damage in dogs chronically infected with *Trypanosoma cruzi*. Acta Trop 161: 44–54, https://doi.org/10.1016/j.actatropica.2016.05.007

Tavernelli LE, Motta MCM, Goncalves CS, da Silva MS, Elias MC, Alonso VL, Serra E, Cribb P (2019) Overexpression of *Trypanosoma cruzi* high mobility group B protein (TcHMGB) alters the nuclear structure, impairs cytokinesis and reduces the parasite infectivity. Sci Rep 9(1): 192, https://doi.org/10.1038/s41598-018-36718-0

Tousoulis D, Psarros C, Demosthenous M, Patel R, Antoniades C, Stefanadis C (2014) Innate and adaptive inflammation as a therapeutic target in vascular disease: the emerging role of statins. J Am Coll Cardiol 63(23): 2491–502, https://doi.org/10.1016/j.jacc.2014.01.054

Viotti R, Alarcón de Noya B, Araujo-Jorge T, Grijalva MJ, Guhl F, Lopez MC, Ramsey JM, Ribeiro I, Schijman AG, Sosa-Estani S, Torrico F, Gascon J, Latin American Network for Chagas Disease, NHEPACHA (2014) Towards a paradigm shift in the treatment of chronic Chagas disease. Antimicrob Agents Chemother 58(2): 635–39, https://doi.org/10.1128/AAC.01662-13

Yu Z, Zou Y, Fan J, Li C, Ma L (2016) Notch1 is associated with the differentiation of human bone marrow-derived mesenchymal stem cells to cardiomyocytes. Mol Med Rep 14(6): 5065–71, https://doi.org/10.3892/mmr.2016.5862

Zhou XL, Zhu RR, Liu S, Xu H, Xu X, Wu QC, Liu JC (2018) Notch signaling promotes angiogenesis and improves cardiac function after myocardial infarction. J Cell Biochem 119(8): 7105–12, https://doi.org/10.1002/jcb.27032

Supporting Information

Additional supporting information may be found online in the Supporting Information section at the end of the article.